Benha Journal of Applied Sciences (BJAS) **print: ISSN 2356–9751**
Vol. (7) Issue 12 (2022), (137-142) **online: ISSN 2356–976x**
http://bjas.bu.edu.eg

SF_6 decomposed products based on AlN nanocage

R. A. Taha, A. S. Shalabi, M. M. Assem, K. A. Soliman*
[1] *Department of Chemistry, Faculty of Science, Benha University, P.O. Box 13518, Benha, Egypt.*
e-mail: kamal.soliman@fsc.bu.edu.eg,

Abstract

SF_6 decomposition products: SO_2, SOF_2, and SO_2F_2 were investigated using $Al_{24}N_{24}$ nanocage based on density functional theory (DFT). The adsorption properties were studied by analyzing adsorption energy, charge transfer, frontier molecular orbitals, and density of states (DOS). Our calculation suggests that the adsorption ability of $Al_{24}N_{24}$ to SO_2 and SOF_2 are stronger than adsorption of SO_2F_2 gas due to chemical adsorption. The results show that $Al_{24}N_{24}$ nanocage plays crucial role for detecting SF_6 decomposition gas with high sensitivity and selectivity.

Keywords: DFT – SF_6 decomposition products - $Al_{24}N_{24}$ nanocage -Adsorption properties

1. The introduction

SF_6 is an excellent gas used in gas insulated switchgear (GIS) and electrical and power system [1, 2, 3] s. Because it has high stability and difficult to decompose. The defects produced during the insulating process leads to partial discharge and caused decomposition of SF_6 gas [4, 5, 6, 7, 8, 9]. The gases that are produced from decomposition such as SO_2, SO_2F_2, SOF_2, H_2S and SOF_4 cause many problems in power system and are harmful to human health [10, 11, 12, 13, 14, 15, 16]. Thus are very important to detect these gases to reduce their damages. Many methods and materials developed to detect these gases [17, 18, 19, 20, 21, 22, 23, 24, 25, 26]. Li et al. used intrinsic MoS_2 and Sc-MoS_2 to detect and adsorbed SF_6 decomposition gases such as H_2S, SO_2F_2, SOF_2 and SO_2 by using DFT calculations and their study show that adsorption of these gases increase by adding Sc as active center atom. The adsorption of SO_2F_2, SOF_2 and SO_2 on Sc-MoS_2 is very strong but H_2S has weak adsorption, so MoS_2 and doped MoS_2 can used as gas sensor to detect SF_6 decomposition gases [27]. Xia et al. used two-dimensional (2D) nanomaterials such as Rh-doped h-BN (Rh-BN) monolayer as a gas sensor to detect SF_6 decomposition gases by using DFT calculation and the results of their calculations show that Rh-BN monolayer is an excellent gas sensor to adsorb and detect SF_6 decomposition gases [28]. Zhang et al. used metal oxide (TiO_2, Fe_2O_3, NiO) cluster-modified single-layer graphene as a gas sensor to adsorb and detect SF_6 decomposition gases by using DFT calculation. Their work show that TiO_2 modification has an excellent adsorption effect for these gases as a gas sensor [29]. Liao et al. used planar 2D material indium triphosphide (InP3) as a gas sensor to detect SF_6 decomposed gases such as SO_2, SOF_2, SO_2F_2 and H_2S by using DFT calculation [30]. Qian et al. used Ga-doped single-walled boron nitride nanotube (Ga-BNNT) as a gas sensor to detect SF_6 decomposition gases such as SOF_2 and SO_2F_2 gases by using DFT calculation. Their results show that by doping the adsorption of these gases increase on Ga-BNNT more than BNNT and the conductivity of SO_2F_2 is better than SOF_2 after the adsorption [31]. Cao et al. used Pt cluster-modified gallium nitride nanotubes (Pt2–GaNNTs) as a gas sensor to detect SF_6 decomposition gases such as H_2S, SO_2, SO_2F_2, and SOF_2 by using DFT calculations. Their study show that the adsorption increases by doping [32]. Liu et al. used Sc-doped WSe_2 monolayers as gas sensors to detect the adsorption and decomposition of gases such as SO_2, SOF_2, and SO_2F_2 by using DFT calculations. Their work show that the adsorption on Sc-WSe_2 is more than WSe_2 [33]. Cui et al. used Pd-doped $PtSe_2$ (Pd-$PtSe_2$) monolayer as a gas sensor to detect and adsorb H_2S and SOF_2 by using DFT calculations and their work show that doped form reduces band gap and increases the adsorption properties more than $PtSe_2$ and the adsorption of SOF_2 on Pd-$PtSe_2$ is better than H_2S gas [34]. Li et al. used Pd-doped MoS_2 (Pd–MoS_2) monolayer as a gas sensor to detect gases such as SOF_2 and SO_2F_2 by using DFT calculations and the results of this work show that Pd–MoS_2 has a good chemical properties to form chemisorption with these gases and it can be used as gas sensor to these gases [35]. Gui et al. used Rh doped MoS_2 to adsorb and detect gases such as SO_2, SOF_2, SO_2F_2 gases by using DFT calculation and their work show that Rh–MoS_2 has adsorption properties more than pristine MoS_2 and the adsorption of SO_2F_2 is less than other gases [36]. In the present study investigate the $Al_{24}N_{24}$ nanocage as a sensing material for SF_6 decomposed products (SO_2, SOF_2, and SO_2F_2) using the density functional theory (DFT). The structural parameters of these gases on the nanocage were determined such as adsorption energy, frontier orbitals, charge transfer using NBO, and density of states.

2. Computational details

DFT calculations were performed for the investigation of adsorption properties of SO_2, SOF_2, and SO_2F_2 gases on the $Al_{24}N_{24}$ nanocage. The optimization of the pristine $Al_{24}N_{24}$ nanocage and adsorption of SO_2, SOF_2, and SO_2F_2 gases on $Al_{24}N_{24}$ nanocage were carried out using the B3LYP level of theory and 6-31g(d) basis set. All calculations utilized Gaussian 09 code [37]. The adsorption energy, charge transfer, NBO analysis and the energy gap parameters were determined.

The adsorption energy (Eads), the charge transfer quantity (Q), and the energy gap (Eg) were calculated from the following equations:

Eads = Egas/$Al_{24}N_{24}$ – Egas – E$Al_{24}N_{24}$

Q = Qads - Qiso

Eg = ELUMO - EHOMO

Where Egas/$Al_{24}N_{24}$, Egas , and E$Al_{24}N_{24}$ are the total energy of gas adsorbed on the nanocage, total energy of gas molecule (SO_2, SOF_2, and SO_2F_2), and the total energy of the $Al_{24}N_{24}$ nanocage respectively. Qads and Qiso are the total charges of of the adsorbed gas molecule and isolated gas respectively.

3. Results and discussion

The optimized structures of SO_2, SOF_2, and SO_2F_2 gas molecules are seen in Fig (**1** and the structure parameters are listed in Fig (**1)** Geometries of SO2, SOF2, and SO2F2 gas molecules

Table (1. The V-shaped structure of SO_2 with S-O bond length 1.46Å that is larger than SOF_2 molecule (1.44Å) and SO_2F_2 molecule (1.43Å) which attributed to increasing electronegativity gradually of S atoms among them. SOF_2 molecule has a triangular structure with S-F bond 1.62 Å and SO_2F_2 exihibit a tetrahedron structure with S-F bond 1.58 Å. Fig(**2**, the optimized structure of $Al_{24}N_{24}$ nanocage and the density of states plot for the $Al_{24}N_{24}$ nanocage shows a significant band gap of 4.09 eV between HOMO and LUMO

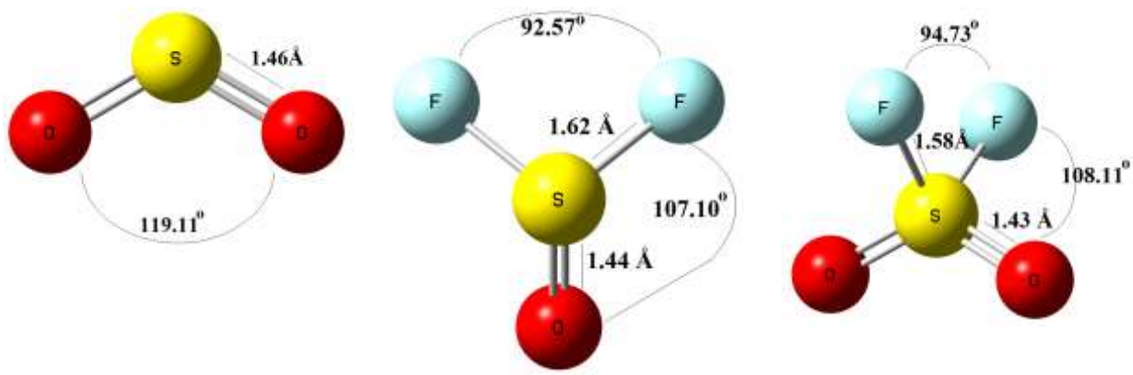

SO2 SOF2 SO2F2

Fig (1) *Geometries of SO2, SOF2, and SO2F2 gas molecules*

Table (1) *structure parameters of SO2, SOF2, and SO2F2 gas molecules*

Gas molecule	Bond length (Å)		Bond angle (°)	
SO_2	S-O	1.46	O-S-O	119.11
SOF_2	S-F	1.62	O-S-F	107.10
	S-O	1.44	F-S-F	92.57
SO_2F_2	S-F	1.58	O-S-F	108.11
	S-O	1.43	F-S-F	94.73

The adsorptions of SF6 decomposed products (SO2, SOF2, and SO2F2 gas molecules) on the Al24N24 nanocage were calculated to analyze the sensitivity of nanocage towards these gas molecules. The optimized configurations of gas molecules on $Al_{24}N_{24}$ nanocage are seen in Fig(**3**. Based on the structural parameters as presented in

Table (**2**, the analysis of the adsorption energy, charge transfer obtained from natural bond orbital (NBO), frontier orbitals, and density of states (DOS) were determined.

For SO_2 system, as shown in Fig(**3**, the S atom of SO_2 molecule interacts with N atom of $Al_{24}N_{24}$ nanocage with a distance 1.68 Å. O atom of SO_2 also interacts with Al atom of nanocage by a distance 1.89 Å and the adsorption energy is -2.58 eV indicating a strong interaction between SO_2 gas molecule and $Al_{24}N_{24}$ nanocage. Furthermore, as listed in Table (**2**, the charge of the adsorbed SO_2 molecule is -0.3 e. This means that the electron was transferred from $Al_{24}N_{24}$ nanocage to SO_2 gas molecule. The distribution of the HOMO and LUMO is displayed in Fig(**3**, and the parameters are determined as listed in

Table (**2**. The HOMO distributed mainly on the six membered ring near SO_2 adsorbed gas and the LUMO distributed on the $Al_{24}N_{24}$ nanocage.

For SOF_2 system, the SOF_2 gas molecule dissociates over the $Al_{24}N_{24}$ nanocage which F atom bind with Al atom of nanocage with bond distance 1.96 Å, S atom interact with N atom of nanocage by a distance 1.63 Å and O atom with Al of nanocage by a distance 1.90 Å. The adsorption energy of SOF_2 molecules on $Al_{24}N_{24}$ nanocage is -5.07 eV. The amount of charge transferred from the $Al_{24}N_{24}$ nanocage to the SOF_2 molecule is -0.32 e. As shown in Fig(**3**,

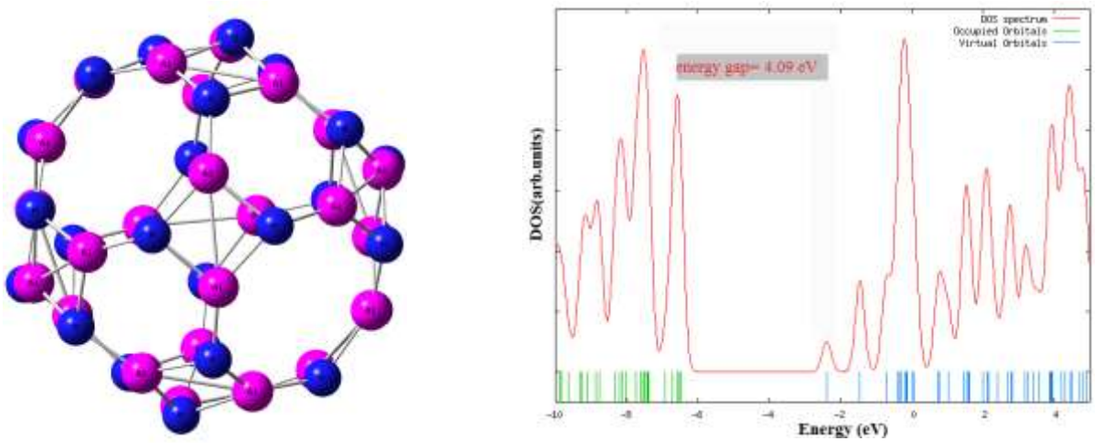

Fig(2) *The optimized structure and DOS of the AL24N24 nanocage.*

Table (2) *The structural parameters of SO2, SOF2, and SO2F2 on the pristine Al24N24 nanocage*

	d (Å)	Eads(eV)	HOMO(eV)	LUMO(eV)	E_g(eV)	Q(e)
$Al_{24}N_{24}$	-	-	-6.48	-2.39	4.09	-
SO_2/ $Al_{24}N_{24}$	1.68 (S-N) 1.89(O-Al)	-2.58	-6.34	-2.40	3.94	-0.30
SOF_2/ $Al_{24}N_{24}$	1.69 (F-Al) 1.63 (S-N) 1.9 (O-Al)	-5.07	-6.15	-2.45	3.7	-0.32
SO_2F_2/ $Al_{24}N_{24}$	2.15 (O-Al)	-0.42	-6.29	-2.27	4.02	0.10

the HOMO distributed on the F atom of SOF_2 and N atom of nanocage and the LUMO distributed on the $Al_{24}N_{24}$ nanocage For SO_2F_2 system, the adsorption of SO_2F_2 on the $Al_{24}N_{24}$ nanocage exhibits a weak interaction. The distance between O atom of SO_2F_2 molecule and the nearst Al atom of nanocage is 2.15 Å and the adsorption energy is -0.42 eV. By analyzing NBO as presented in

Table **(2**, we found that the charge on SO_2F_2 after adsorption on nanocage is 0.1 e which indicates the charge transfer from the SO_2F_2 molecule to the nanocage. As seen in Fig(3) adsorption configuration and frontier orbitals of SO2, SOF2, and SO2F2 on the Al24N24 nanocage., the HOMO is distributed around on the $Al_{24}N_{24}$ nanocage while the LUMO distributed on the whole system. The comparison between the three SF_6 decomposed products shows that the adsorption energy value for SO_2F_2 system is smaller than SO_2 and SOF_2 systems, and the electron transfer manifests the occurrence of strong chemisorption in SO_2 and SOF_2 adsorption system.

Fig(4 shows the DOS plots after the adsorption of SO_2, SOF_2, and SO_2F_2 on the $Al_{24}N_{24}$ nanocage. As shown in Fig 5 and Table 2 the $Al_{24}N_{24}$ nancocage has a minimum LUMO of -2.39 eV and a maximum HOMO of -6.48 eV. Upon adsorption of SO_2, SOF_2, and SO_2F_2 on the $Al_{24}N_{24}$ nanocage, it can be inferred that a significant effect on the electronic properties of the $Al_{24}N_{24}$ nanocage occurs. As presented in

Table **(2**, the $Al_{24}N_{24}$ nanocage has a LUMO of -2.39 eV while for SO_2, SOF_2, and SO_2F_2 on the $Al_{24}N_{24}$ nanocage are -2.40 eV, -2.45 eV, and -2.27 eV respectively. The band gap decreases significantly for SO_2, and SOF_2 on the $Al_{24}N_{24}$ nanocage implying the chemisorption of these gases on the nanocage.

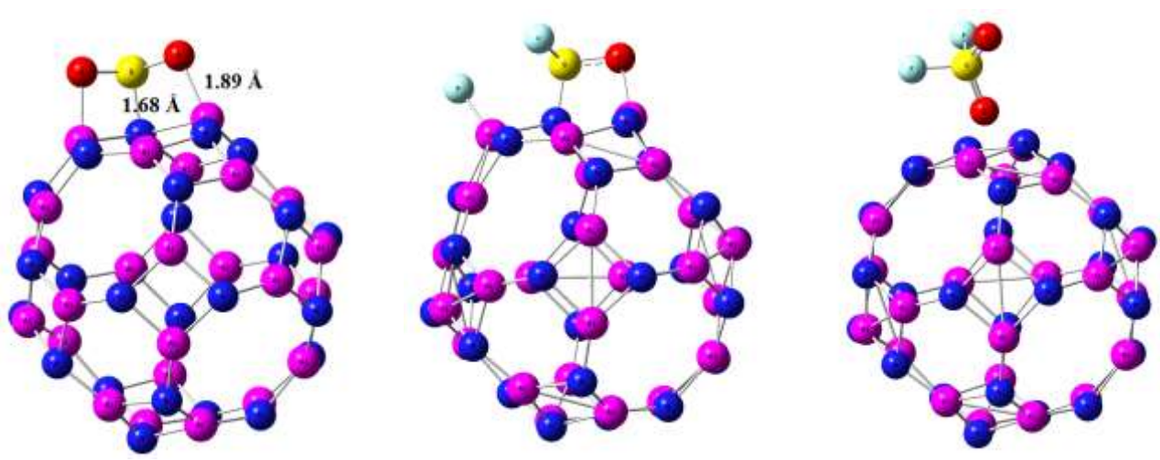

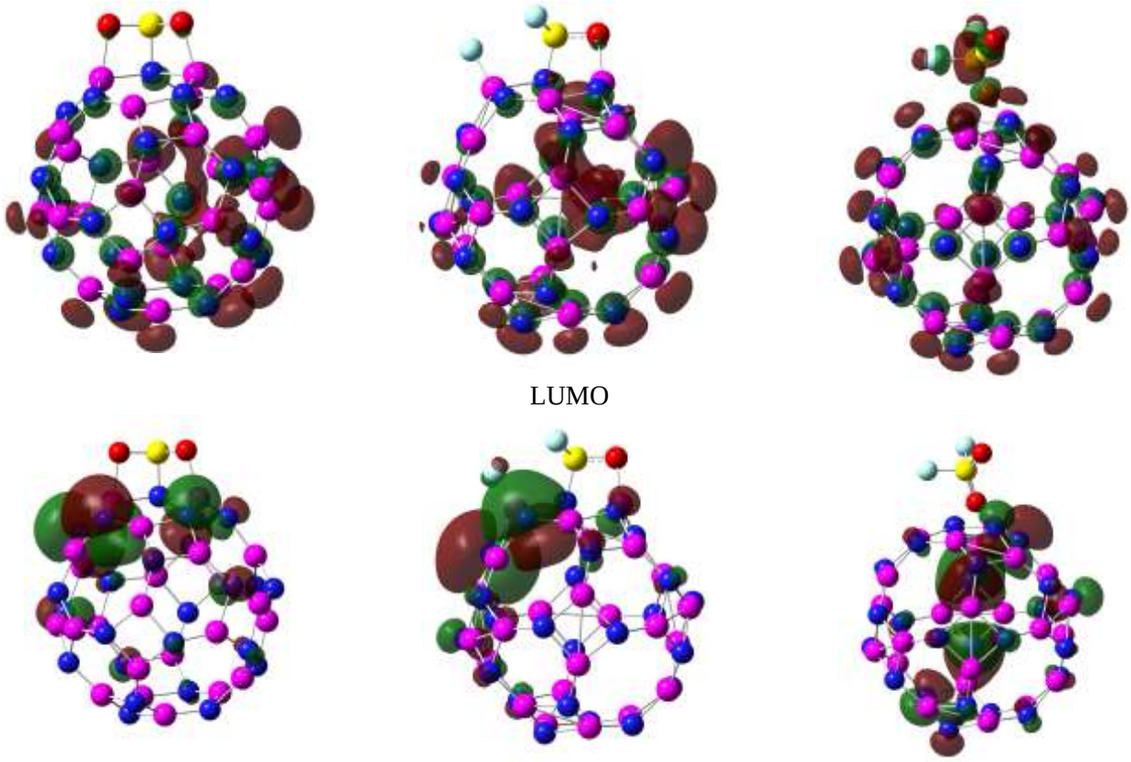

Fig(3) *adsorption configuration and frontier orbitals of SO2, SOF2, and SO2F2 on the Al24N24 nanocage.*

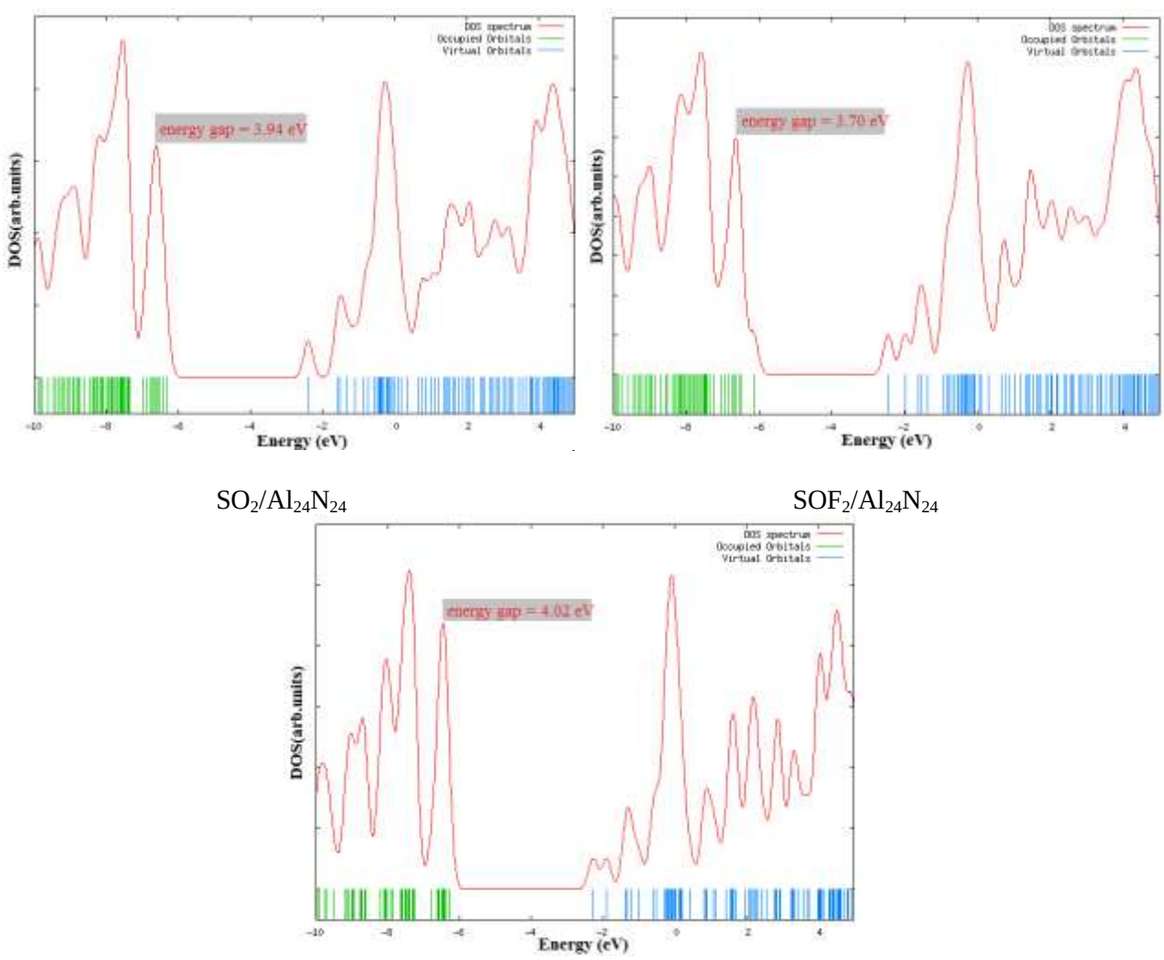

$SO_2/Al_{24}N_{24}$ $SOF_2/Al_{24}N_{24}$

$SO_2F_2/Al_{24}N_{24}$

Fig(4) *DOS plots of SO2, SOF2, and SO2F2 on the Al24N24 nanocage.*

The desorption time represents an important factor for gas sensing material. The desorption time can be calculated by the following equation

$$\tau = A^{-1} e^{E_a/K_B T}$$

Where A is the apparent frequency factor (10^{12} s^{-1}), K_B, T are the Boltzmann's constant, and the tested temperature respectively. The E_a represent the potential barrier of the desorption process and the value equal to Eads. The desorption property of the three gases (SO_2, SOF_2, and SO_2F_2) on the $Al_{24}N_{24}$ nanocage were extra-long desorption time for the SO_2, and SOF_2 gas molecules but short desorption time for SO_2F_2 gas molecule. Therefore, $AL_{24}N_{24}$ nanocage can be selected as adsorbents to SO_2 and SOF_2 gas molecules because of long desorption time at room temperature.

4. Conclusion

In the present study investigate the $Al_{24}N_{24}$ nanocage as a sensing material for SF_6 decomposed products (SO_2, SOF_2, and SO_2F_2) using the density functional theory (DFT). The structural parameters of these gases on the nanocage were determined such as adsorption energy, frontier orbitals, charge transfer using NBO, and density of states. The results reveals that the adsorption of SO2 and SOF2 gases are chemisorption on the $Al_{24}N_{24}$ nanocage, while SO_2F_2 gas is physisorbed on the nanocage which can be desorbed easily.

References

[1] A.P. Purnomoadi, A.R. Mor and J.J. Smit, Spacer flashover in Gas Insulated Switchgear (GIS) with humid SF6 under different electrical stresses. International Journal of Electrical Power & Energy Systems.vol.116,pp.105559,2020.

[2] L. Liu, Y. Zheng, Y. Hao, Q. Zhang , X. Li, L. Chen and L. Li, Surface flashover patterns of GIS basin insulator under impulse voltage. Engineering Failure Analysis,vol. 130,pp.105800,2021.

[3] Th.A. Paul, M. Porus, B. Galletti and A. Kramer, SF6 concentration sensor for gas-insulated electrical switchgear. Sensors and Actuators A: Physical,vol.206,pp.51-56, 2014.

[4] B. Niu, F. Ma, S. Sun and Y. Xu, Research on operation and fault diagnosis technology for EHV/UHV SF6 circuit breakers pre-insertion resistors. Energy Reports,vol.7,pp. 38-47,2021.

[5] F. Zeng, Z. Lei, X. Yang, J. Tang, Q. Yao and Y. Miao, Evaluating DC Partial Discharge With SF6 Decomposition Characteristics. IEEE Transactions on Power Delivery,vol.34(4),pp.1383-1392, 2019.

[6] M. Ren, B. Song, T. Zhuang and S. Yang, Optical partial discharge diagnostic in SF6 gas insulated system via multi-spectral detection. ISA Transactions,vol.75,pp.247-257,2018.

[7] H.N. Afrouzi, A. Hassan, D.T.Y. Chee, K. Mehranzamir, Z.A. Malek, S.V. Mashak and J. Ahmed, In-depth exploration of partial discharge modelling methods within insulations. Cleaner Engineering and Technology,vol.6,pp.100390,2022.

[8] S. Wu, F. Zeng, J. Tang, Q. Yao and Y. Miao, Triangle Fault Diagnosis Method for SF6 Gas-Insulated Equipment. IEEE Transactions on Power Delivery,vol.34(4) ,pp.1470-1477,2019.

[9] X. Zhang, J.Ren, J. Tang and C.Sun, Kernel statistical uncorrelated optimum discriminant vectors algorithm for GIS PD recognition. IEEE Transactions on Dielectrics and Electrical Insulation,vol. 16(1),pp. 206-213,2009.

[10] F.Y.Chu and R.E.Massey, THERMAL DECOMPOSITION OF SF6 AND SF6-AIR MIXTURES IN SUBSTATION ENVIRONMENTS, in Gaseous Dielectrics III, L.G. Christophorou, Editor., Pergamon. pp.410-419,2013.

[11] K. L. Seaward, N. J. Moll and W. F. Stickle, Surface contamination and damage from CF4 and SF6 reactive ion etching of silicon oxide on gallium arsenide. Journal of Electronic Materials,vol.19(4),pp.385-391,1990.

[12] H.Nishino, N. Hayasaka and H. Okano, Damage-free selective etching of Si native oxides using NH3/NF3 and SF6/H2O down-flow etching. Journal of applied physics,vol.74(2),pp.1345-1348,1993.

[13] C.Liu, S.Palanisamy, S.Chen, P.Wu and L.Yao, Mechanism of Formation of SF6 Decomposition Gas Products and its Identification by GC-MS and Electrochemical methods: A mini Review. Int. J. Electrochem. Sci,vol.10(5),pp.4223-4231,2015.

[14] C.T. Dervos, and P. Vassiliou, Sulfur hexafluoride (SF6): global environmental effects and toxic byproduct formation. Journal of the Air & Waste Management Association,vol.50(1),pp.137-141,2000.

[15] W.T.Tsai, The decomposition products of sulfur hexafluoride (SF6): Reviews of environmental and health risk analysis. Journal of Fluorine Chemistry,vol.128(11) pp.1345-1352,2007.

[16] Y.F.Wang, M.Shih, C.H.Tsai and P.J.Tsai, Total toxicity equivalents emissions of SF6, CHF3, and CCl2F2 decomposed in a RF plasma environment. Chemosphere,vol.62(10),pp.1681-1688, 2006.

[17] X.Dong, X.Zhang, H.Cui and J.Zhang., A first principle simulation of competitive adsorption of SF6 decomposition components on nitrogen-doped anatase TiO2 (101) surface. Applied Surface Science,vol.422,pp.331-338,2017.

[18] X.Zhang, L.Yu, Y.Gui and W.Hu, First-principles study of SF6 decomposed gas

adsorbed on Au-decorated graphene. Applied Surface Science,vol.367,pp.259-269,2016.

[19] Y.Gui, H.Sun, H.Wei, S.Duan, C.Tang and X.Zhang, Effect of Nickel Doping on Adsorption of SF6 Decomposition Products over MoS2 Surface. JOM,vol.71(11),pp. 3971-3979,2019.

[20] H.Qian, W.Lu, X.Wei, W.Chen and J.Deng, H2S and SO2 adsorption on Pt-MoS2 adsorbent for partial discharge elimination: A DFT study. Results in Physics,vol.12,pp. 107-112,2019.

[21] H.Suman, R.Srivastava, S.Shrivastava, A.Srivastava, A.P.Jacoba and C.S.Malvi, DFT analysis of H2S adsorbed zigzag and armchair graphene nanoribbons. Chemical Physics Letters,vol.745,pp.137280,2020.

[22] S.Xu, Y.Zhang, F.Xu, C.Chen and Z.Shen, Theoretical study of the adsorption behaviors of gas molecules on the Au-functionalized MoS2 nanosheets: A search for highly efficient gas sensors. Computational and Theoretical Chemistry,vol.1188,pp.112935,2020.

[23] Q.Zhou, W.Ju, X.Su, Y.Yong and X.Li, Adsorption behavior of SO2 on vacancy-defected graphene: A DFT study. Journal of Physics and Chemistry of Solids,vol.109 ,pp. 40-45, 2017.

[24] Y.Gui, D.Liu, X.Li, C.Tang and Q.Zhou, DFT-based study on H2S and SOF2 adsorption on Si-MoS2 monolayer. Results in Physics,vol.13, pp.102225,2019.

[25] H. Huang, Y. Yu and M. Zhang, Analysis of adsorption properties of SF6 decomposed gases (SOF2, SO2F2, SF4, CF4, and HF) on Fe-doped SWCNT: A DFT study. Applied Surface Science,vol.505,pp.144622,2020.

[26] K.Xu, N.Liao, B.Zheng and H.Zhou, Adsorption and diffusion behaviors of H2, H2S, NH3, CO and H2O gases molecules on MoO3 monolayer: A DFT study. Physics Letters A, vol.384(21),pp.126533, 2020.

[27] B.Li, Q.Zhou, R.Peng, Y.Liao and W.Zeng, Adsorption of SF6 decomposition gases (H2S, SO2, SOF2 and SO2F2) on Sc-doped MoS2 surface: A DFT study. Applied Surface Science,vol.549,pp.149271,2021.

[28] S.Y.Xia, L.Q.Tao, T.Jiang, H.Sun and J.Li, Rh-doped h-BN monolayer as a high sensitivity SF6 decomposed gases sensor: A DFT study. Applied Surface Science,vol.536,pp.147965,2021.

[29] Q.Zhang, YGui, H.Qiao, X.Chen and L.Cao, Theoretical study of SF6 decomposition products adsorption on metal oxide cluster-modified single-layer graphene. Journal of Industrial and Engineering Chemistry,vol.105,pp. 278-290,2022.

[30] Y.Liao, Q.Zhou, R.Peng and W.Zeng, Adsorption properties of InP3 monolayer toward SF6 decomposed gases: A DFT study. Physica E: Low-dimensional Systems and Nanostructures,vol.130,pp. 114689, 2021.

[31] H.Qian, J.Deng, H.Zhou, X.Yang and W.Chen, A DFT study on the adsorption of Ga-BNNT to SF6 decomposition products under partial discharge. Results in Physics, vol.14,pp.102419, 2019.

[32] W.Cao, Y.Gui, T.Chen, L.Xu and Z.Ding, Adsorption and gas-sensing properties of Pt2–GaNNTs for SF6 decomposition products. Applied Surface Science, vol.524 ,pp. 146570,2020.

[33] Y.Liu, J.Zhou, L.Xu, J.Long, Q.Cheng and W.Zeng, Sc doped WSe2 monolayer: a candidate for enhanced adsorption and detection of SF6 decomposition gases. Journal of Materials Research and Technology,vol.17, pp.1786-1798,2022.

[34] H.Cui, Y.Guo, Q.Zhao and G.Zhang, Pd-doped PtSe2 monolayer with strain-modulated effect for sensing SF6 decomposed species: a first-principles study. Journal of Materials Research and Technology, vol.18, pp. 629-636,2022.

[35] T.Li, Y.Gui, W.Zhao, C.Tang and X.Dong, Palladium modified MoS2 monolayer for adsorption and scavenging of SF6 decomposition products: A DFT study. Physica E: Low-dimensional Systems and Nanostructures,vol.123, pp.114178,2020.

[36] X.Gui, Q.Zhou, S.Peng, L.Xu and W.Zeng, Adsorption behavior of Rh-doped MoS2 monolayer towards SO2, SOF2, SO2F2 based on DFT study. Physica E: Low-dimensional Systems and Nanostructures,vol.122 pp.114224,2020.

[37] M.J. Frisch, G.W. Trucks, H.B. Schlegel, G.E. Scuseria, M.A. Robb, J.R. Cheeseman, G. Scalmani, V. Barone, B. Mennucci, G.A. Petersson, H. Nakatsuji, M. Caricato, X. Li, H.P. Hratchian, A.F. Izmaylov, J. Bloino, G. Zheng, J.L. Sonnenberg, M. Hada, M. Ehar.